Functional Materials 19, No.1 (2012)

Researches and developments on production of Ni–W alloy based substrates for second generation high-temperature superconductors

V.A.Finkel, A.M.Bovda, V.V.Derevyanko, S.A.Leonov, M.S.Sungurov, T.V.Sukhareva, V.M.Khoroshikh, Yu.N.Shakhov

National Scientific Center "Kharkiv Institute of Physics and Technology", National Academy of Sciences of Ukraine, 1 Akademicheskaya St., 61108 Kharkiv, Ukraine

Received October 21, 2011

The possibilities to prepare high-quality substrates for second generation high temperature superconductors based on Ni–W alloys in the 0–9.5 at. % W concentration range was studied. Researches and developments were carried out in the following directions: a) Ni–W alloy synthesis; b) preparation of Ni–W alloy tapes by rolling with subsequent heat treatment; c) coating the tape by TiN layer. For the first time, the possibility was established to obtain the {001} <100> cubic texture favour to $YBa_2Cu_3O_{7-\delta}$ superconductor subsequent epitaxial growth on the high W paramagnetic Ni–W tape surface by varying the regimes of TiN deposition.

Изучены возможности получения высококачественных подложек для ВТСП-проводников второго поколения на основе сплавов Ni–W в диапазоне концентрации вольфрама 0–9.5 ат. %. Исследования и разработки проводились в следующих основных направлениях: а) синтез сплавов Ni–W; б) получение ленты из сплавов Ni–W путем прокатки и последующей термообработки; в) нанесение буферного слоя TiN на поверхность ленты. Впервые установлена возможность получения кубической текстуры {001} <100>, благоприятствующая последующему эпитаксиальному росту слоев сверхпроводника $YBa_2Cu_3O_{7-\delta}$ на поверхности ленты из парамагнитных сплавов Ni–W с высоким содержанием вольфрама путем изменения режимов нанесения покрытий на основе TiN.

1. Introduction

As it is known [1, 2], the architecture of new generation tape high-temperature superconductors (2G HTS tapes) with crucial current density $j_c \sim 10^6$ A/cm^2 at liquid nitrogen temperature (77.4 K) is rather complex. Practically always, the following three main components present in the HTS conductor:

1) a base (a thin tape from Ni–W alloy with different compositions, or rarer, Hastelloy, stainless steel, etc.);

2) non-superconducting buffer layer/layers (oxides, nitrides, etc);

3) a superconducting $YBa_2Cu_3O_{7-\delta}$ film coating (for 2G HTSC, this is a thin textured $YBa_2Cu_3O_{7-\delta}$ layer).

The value of the transport current I flowing without dissipation through the HTS conductor, depends not only on the $YBa_2Cu_3O_{7-\delta}$ film critical current density j_c, but to a great extent, is determined by the structure, magnetic and mechanical properties of the metallic tape — the substrate for the buffer layer and HTS tapes [3].

From the materials practically used as substrates for HTS tapes preparation, the most promising are the FCC lattice nickel-tungsten alloys in the composition range

from 0 to ~ 9.5 at. % W due to their high mechanical properties. The Ni–W alloys are synthesized using powder metallurgy [4], induction melting [3, 5], electrolytic deposition [6], etc. Note, that the information on extreme methods of Ni–W alloy synthesis giving a possibility to modify the macro- and microstructure of the ingots is practically absent in the literature. As initial substances for Ni–W alloy synthesis, the high-purity Ni and W powders are used.

The effectiveness of Ni–W alloy tapes as 2G HTS tapes components is substantially influenced by the alloy magnetic structure (collinear ferromagnetic one at low W content, or paramagnetic one — at high W [7, 8]), as well, by substrate crystallographic texture formed during mechanical and subsequent heat treatment of the tape [9–13]. To provide the high current-carrying ability for 2G HTSC, the most favour is the {100} <001> type cubic structure (see, e.g. [3, 4, 7]) giving the possibility of superconductor layer epitaxial $\{100\}_{Ni-W} \parallel \{100\}_{YBa_2Cu_3O_{7-\delta}}$ growth.

Recently, titanium nitride TiN with NaCl type FCC lattice is considered as a rather promising material for buffer layers [3, 14, 15] (along with "traditional" Y_2O_3, CeO_2, etc.), due to the possibility to monitor the TiN layer texture (and as a consequence, the texture of $YBa_2Cu_3O_{7-\delta}$ HTSC film coated onto the TiN layer) varying the coating regimes. The objective of the work is development of optimum ways to prepare high-quality substrates based on Ni–W alloys in the W concentration range 0–9.5 at. % for 2G HTS tapes. Also, the never before considered possibility of texture monitoring in high W containing Ni–W alloy thin tapes by varying the TiN coating regimes is studied.

To achieve the aim, the program of investigations and developments was realized in following stages:

— thorough purification of Ni and W powders from gaseous impurities;

— compacting the Ni and W powders with various compositions;

— smelting Ni–W alloys in vacuum (thermal heating) or vacuum arc-smelting followed by quenching from liquid phase;

— rolling the Ni–W ingots with intermediate annealing for preparing the tape with set sizes;

— mechanical and chemical polishing the Ni–W alloy tape;

— final high-temperature annealing the Ni–W tape;

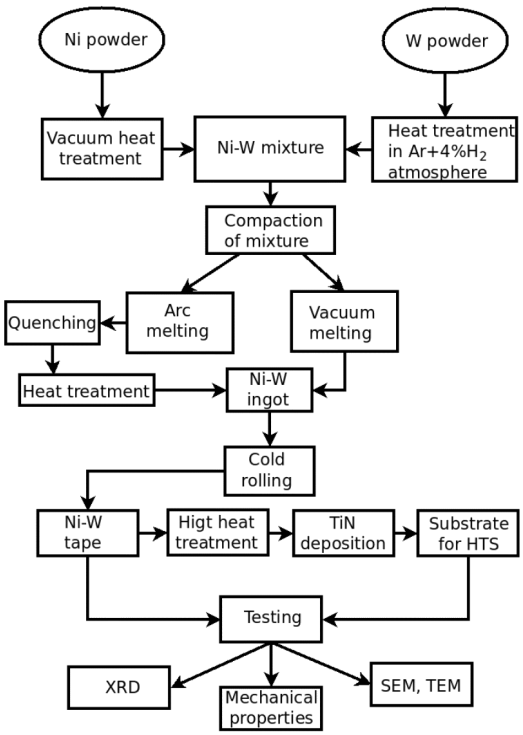

Fig. 1. The scheme of producing the Ni–W alloys substrates with TiN coating. Shortenings: XRD — X-ray diffraction analysis; SEM — scanning electron microscopy; TEM — transmission electron microscopy.

— coating the Ni–W tape with TiN thin layers;

— validation of the tape before and after TiN coating.

The scheme of the N–W substrate preparation with TiN coating for HTS tapes deposition is shown in Fig. 1.

2. Results and discussion

The given below results of researches and developments in three main directions of the work on creation of high quality substrates for 2G HTSC are following: synthesis of Ni–W alloys, preparation of tapes from Ni–W alloys, and deposition of TiN thin layers onto Ni–W tapes.

2.1. Synthesis of Ni–W alloys

The initial materials for obtaining the Ni–W alloys were the Ni and W powders with 99.98–99.99 % purity (by metallic impurities). In such powders, the main impurity is oxygen present as nickel and tungsten oxides.

As it is known, the NiO decomposes in elements in the temperature range from 330

to 850°C [16]. For purification of Ni powder from gaseous impurities the heat treatment at temperatures higher 850°C was used.

For refinement of W powder from oxygen in numerous oxides, the high-temperature treatment (from ~1000 to 1200°C) in reducing Ar + 4 % H_2 gaseous mixture flow [4] was applied. The refinement was carried out in the specially made tube furnace, through which the gaseous mixture flux was passed at the pressure somewhat higher than atmospheric one. Attempts to use chemical methods for W powder purification from oxides were found to be less effective.

After refinement from gaseous impurities, the Ni and W powders were thoroughly mixed in necessary proportions (from 0 to 9.5 at. % W) using mill-mortar "*Pulverizette*". Then the powder mixtures were pressed in pellets for subsequent melting.

2.1.1. Vacuum melting of Ni–W alloys

The Ni–W alloys were synthesized using thermal heating in deep vacuum ($p \sim 10^{-6}$ Torr) in the resistance furnace with molybdenum wind placed in large volume vacuum chamber (system "*VUM*" [17]). The pressed pellets of ~ 50 g mass were put into horizontal alundum crucibles ("boats"). The melting was carried out at ~ 1550°C temperature, beyond liquidus line (1515°C) in Ni–W phase diagram for maximum tungsten content [18], during several hours with subsequent slow cooling.

2.1.2. Arc-melting of Ni–W alloys

The arc-melting of the various compositions Ni–W alloy pressed pellets with mass up to ~ 50 g was realized in the vacuum arc-furnace with permanent tungsten electrode [19]. To provide the ingot homogeneity, they were three-times melted and overturned. At every stage of the melting, the sample mass changes were controlled.

Formation of the work material for rolling was done in the "*Lenta*" facility in argon atmosphere [20]. For argon purification, directly before the sample melting, the remelting of a zirconium ingot placed in the same bulk copper crystallizer was fulfilled. The arc current was ~ 300 A, and the excess pressure in the smelting chamber was 0.5 kg/cm^2. The melt with mass up to ~ 50 g was poured in the specially developed slit-like water-cooled copper crystallizer.

The slit-like crystallizer consists of two chambers — upper and bottom ones, separated by the refractory outflow jet. In the upper chamber, the sample is melted, and then the melt passes through the refractory outflow jet into the copper crystallizer for cooling.

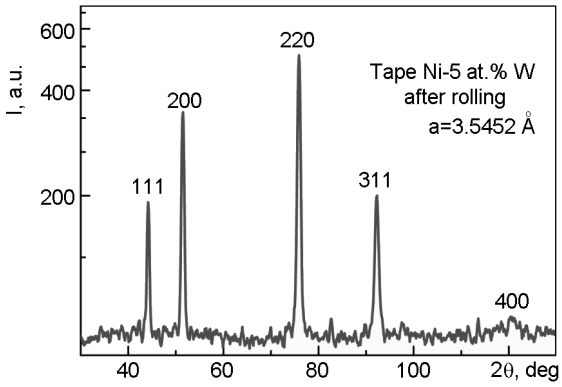

Fig. 2. X-ray diffraction pattern of Ni — 5 at. % W alloy tape after cold rolling. Diffractometer DRON-UM-1. $Cu_{K\alpha}$ irradiation.

Varying the melt overheating level and the pressure over smelt it is possible to regulate the cooling rate. The sample prepared in such way looks like a parallelepiped with sizes, allowing mechanical treatment — rolling — using routine equipment.

2.2. Production and treatment of Ni–W alloy tape

The ingots prepared by vacuum- or arc-melting were used for production of Ni–W alloy tapes with various compositions. As a rule, the alloy workpiece thickness was ~ 5 mm, and the final tape thickness d ~ 100 μm. Traditional methods of room temperature rolling were applied (see, e.g. [3–5, 17, 21]) using the multifold rolling mill.

It is known that the rolling of nickel and their alloys including the Ni–W alloys presents great difficulties caused by high level stress arising under deformation process. In this connection, under cold rolling, as a rule, it is necessary to alternate the "deformation — annealing" cycles [22]. The researches have shown, that the optimal regime for the cold rolling of the Ni–W alloys with W content up to 9.5 at. % is the cycle "~ 10 % deformation — intermediate 600°C/1 h vacuum annealing".

In Fig. 2 the X-ray diffraction pattern of Ni — 5 at. % W alloy tape with thickness d ~ 100 μm produced by the similar cycle rolling processing is shown. Only the formation of the strain texture similar to β-brass type {110} <112> is revealed [23]. The texture character does not depend substantially on

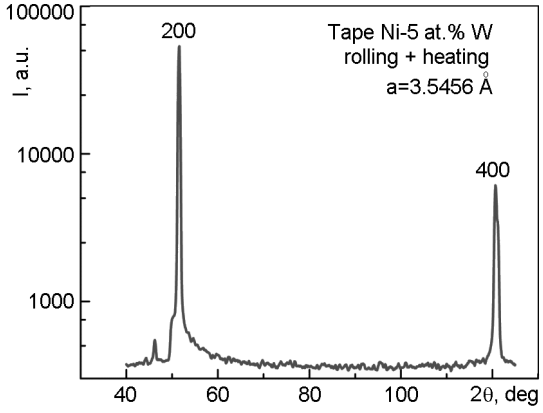

Fig. 3. X-ray diffraction pattern of Ni — 5 at. % W alloy tape after cold rolling and vacuum annealing (1000°C/2 h). Diffractometer DRON-UM-1. $Cu_{K\alpha}$ irradiation.

the alloy composition. Further, the mechanical and/or chemical polishing the tape surface were made.

The resulting operation during the Ni–W alloy tape production was the high-temperature annealing (the scheme is shown in Fig. 1). The necessary conditions of the final heat treatment were established as following: 1000–1200°C/1–2 h. As a result, the recrystallization {001} <100> cubic texture is formed which is favorable to subsequent epitaxial growth of $YBa_2Cu_3O_{7-\delta}$ superconductor (see above). From the X-ray diffraction pattern of Ni — 5 at. % W alloys after the rolling and the last annealing shown in Fig. 3, it is seen that the recrystallization texture has quite high perfection.

The obtained results of structure investigations support the well known fact that in Ni–W tapes with high W content the cubic texture is not formed after high-temperature annealing (see e.g. [8–12]). Usually, this effect is considered to be connected with lowering stacking fault energy in the alloys as the W content increases [24]. In the next section, some possibilities to create the cubic texture in Ni — 9.5 at. % W alloy thin tapes will be discussed.

The main results on researching the following mechanical properties of Ni–W alloy tapes with various compositions: yield stress, σ_f, ultimate stress, σ_b, and the relative extension, δ, are given in Table 1. The evident effects of increased yield stress and ultimate stress under increasing W content in the alloys are revealed.

2.3. Deposition of TiN thin layers onto Ni–W alloy tape

For deposition of titanium nitride coating onto the Ni–W tape surface, the method of substance condensation from plasma flux generated by low pressure arc was applied [25].The method allows treating the surface by high-energy ions extracted from the plasma by supplying high potential U onto the surface; that provides the sample surface layer effective cleaning from contaminations and impurities and causes high adhesion properties of the coatings. Introduction of chemically active gases into the work volume permits to obtain the coatings of various compositions — nitrides, oxides etc. High rate of the chemical reactions is caused by the presence of metallic ions in the condensation zone as well as gaseous atoms and molecules activated during interactions with plasma ions and electrons.

The main disadvantage limiting application of the vacuum-arc method for TiN coating deposition onto the Ni–W alloy tapes used as substrates for 2G HTSC is the presence of macro-particles-drops and solid pieces of the cathode material in the plasma flux. Such defects can impede the flow of dissipation-free superconduction current. For removing the macro-particles from the condensation material flux during their movement from cathode to plasma source exit, different electromagnetic systems for charged particle turning are applied [26, 27]. However, the plasma filters developed to date are characterized by low coefficient of working material utilization, as well as are bulky and high expensive.

An alternative to the method of coating deposition using plasma filters may be the technique of deposition under higher working gas pressures ($p_N > 1$ Pa). At such pres-

Table 1. Mechanical properties of Ni–W alloy tapes at room temperature

Alloy composition	σ_f, kg/mm^2	σ_b, kg/mm^2	δ, %
Ni	8.7	28.5	20.0
Ni-5 at. % W	20.0	58.7	36.0
Ni-7.5 at. % W	26.3	69.6	35.4
Ni-9.5 at. % W	33.7	82.1	29.7

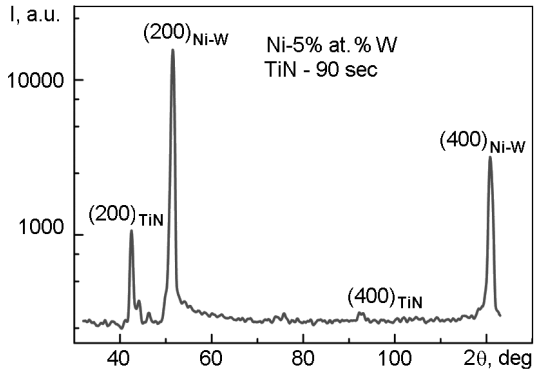

Fig. 4. X-ray diffraction pattern of Ni — 5 at. % W alloy tape with TiN coating. Diffractometer DRON-UM-1. $Cu_{K\alpha}$ irradiation.

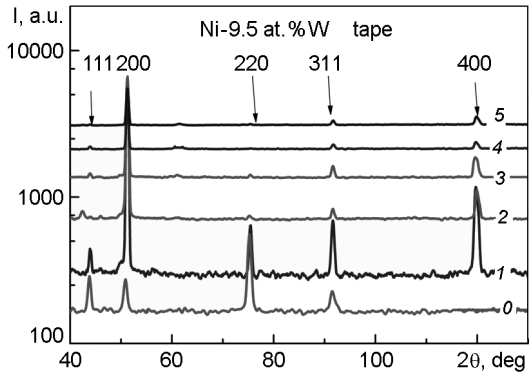

Fig. 5. X-ray diffraction pattern of Ni — 9.5 at. % W alloy tape. *0* — after rolling; *1* — after vacuum high temperature annealing; *2* — after TiN coating deposition (deposition time τ_{TiN} = 60 s); *3* — after TiN coating deposition (deposition time τ_{TiN} = 120 s); *4* — after TiN coating deposition (deposition time τ_{TiN} = 420 s); *5* — after TiN coating deposition (deposition time τ_{TiN} = 900 s). Diffractometer DRON-UM-1. $Cu_{K\alpha}$ irradiation. Above: FCC lattice indices of Ni — 9.5 at. % W alloy.

sures, the deposition is occurred from randomized plasma flux including out of the direct vision zone of the plasma source cathode (substrate underside). This fact allows producing the drop-free coatings with rather high deposition rates (10–100 μm/h) without application of any systems of the plasma separation [28].

Under such pressures, the coating deposition takes place from the randomized plasma flux including outside the direct vision zone of the plasma source cathode (substrate underside). This fact allows producing drop-free coatings with rather high deposition rate without application of plasma separation systems.

In the experiments on deposition of TiN thin layers onto the Ni–W alloy tape surface, VT-1 grade titanium was used for the cathode material. In a series of the experiments, the Ni — 5 at. % W and Ni — 9.5 at. % W alloys tape samples with thickness d ~ 100 μm were studied. The samples looked like as two plates closely pressed to one another that gave an opportunity to investigate the structure and properties of exterior and shady surfaces (drop-free regime), as well as the interior sides of these surfaces. The samples were positioned in the center of the vacuum chamber, at the axis of the positioning fixture, and have the possibility to revolve on the normal to surface axis. The treatment regimes for the samples of this experiment series on titanium nitride layer deposition are given in Table 2.

In Fig. 4, a typical X-ray diffraction pattern is shown for the Ni — 5 at. % W alloy tape sample with TiN coating (deposition time τ = 90 s).

Two systems of diffraction lines are observed: the FCC lattice lines of Ni — 5 at. % W alloy (a = 3.5436 Å), and the lines of Nail-type lattice belonging to TiN compound (a = 4.2741 Å). For both phases, the presence of open cubic texture {001} <100> is characteristic.

Table 2. Regimes for TiN deposition onto Ni — 5 at. % W alloy tape surfaces

Substrate negative potential U, V	Arc current I, A	Nitrogen pressure p_N, Pa	Deposition time τ_{TiN}, s	Notes
300	80	2.4	15	
300	80	2.4	30	
300	80	2.4	90	
300	80	2.4	90	Samples revolved
300	80	2.4	300	
300	80	2.4	900	

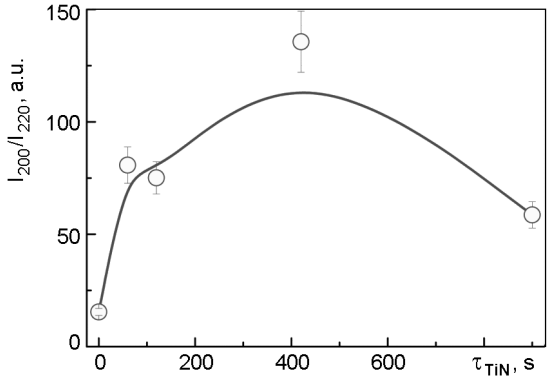

Fig. 6. The intensity ratio of (200) and (220) diffraction lines versus TiN layer deposition time onto Ni — 9.5 at. % W alloy tape.

The diffraction pattern evolution for Ni — 9.5 at. % W alloy tape as a result of annealing and TiN layer deposition is show in Fig. 5.

It is observed that, as the TiN coating deposition time (τ_{TiN}) increase, in other words, as the TiN thickness, d_{TiN}, grows, the relative intensities of (h 0 0) type diffraction lines increase, while the intensities of reflections from diagonal (h h 0) and other FCC lattice planes decrease. Such character of the diffraction pattern evolution indicates *qualitatively* the substantial intensification of {001} <100> type cubic texture degree in the Ni — 9.5 at. % W paramagnetic alloy tape.

Very informative was the behaviour of the cubic (h 0 0) and diagonal (h h 0) diffraction line intensity ratio, $I_{200}(\tau_{TiN})/I_{220}$, characterizing the cubic texture degree depending on the deposition time (Fig. 6). As it is observed, the {001} <100> texture evolution degree rises steeply with increasing deposition time, τ_{TiN}, and the maximum extent is achieved at τ_{TiN} close to the layer thickness ~ 1.5 μm. Obviously, the mechanical stresses occurring in the system "Ni — 9.5 at. % W alloy tape — TiN coating" result in the cubic texture intensification, and at certain TiN layer thickness, the optimum conditions for {001} <100> type texture formation are realized. In our case, such the conditions seem to appear near ~ 1.5 μm.

The important fact is worth to note that the data shown in Figs. 5 and 6 concern the tape produced by rolling of the vacuum melted Ni — 9.5 at. % W alloy. The effects of the recrystallization texture formation under high temperature annealing and influence of the TiN deposited layers in the Ni — 9.5 at. % W alloy tapes prepared by arc-smelt, quenching and subsequent annealing are substantially smaller.

3. Conclusions

Thus, the aim of the work achievement was reduced to developing the creation strategy of the substrates — buffer coated Ni–W alloy tapes, combining the crystallographic texture favour for epitaxial growth of $YBa_2Cu_3O_{7-\delta}$ HTSC layers, and absence of ferromagnetism resulting in decreased density of superconducting current flowing in the HT-superconductor. The serious obstacle for creation of the substrates with such combination of texture (namely, {001} <100> type cubic texture) and paramagnetism is low energy of the stacking faults hindering from the cubic texture formation in the paramagnetic high W content Ni–W alloy tapes. On the same account, there takes place the "giant" yield stress with increasing W content in N–W alloys, and as a result, heavy hardening under cold deformation making difficult the rolling process.

The results of researches and developments carried out in abovementioned three main directions — Ni–W alloy metallurgy (section 2.1), rolling and heat treatment of Ni–W alloy tapes (section 2.2), TiN layer deposition onto the tape by condensation from plasma flux (section 2.3), — indicates the possibility to made sufficiently perfect substrates for 2G HTSC which combine the crystallographic texture favorable to HTSC film epitaxial growth, the paramagnetic state of the matrix, and the effective buffer layer.

One should consider, that optimization of conditions for Ni–W alloy melting, the tape preparation and heat treatment, and the TiN buffer layer deposition will give the possibility of scale production of substrates for 2G HTSC.

The work is done under support of Ukrainian Science and Technology Center (Project STCU # P424).

References

1. D.Larbalestier, A.Gurevich, D.M.Feldmann, A.Polyanski, *Nature*, **41**, 368 (2001).
2. G.Celentano, V.Galluzzi, A.Maneiani et al., *J. Phys.:Conf. Ser.*, **43**, 158 (2006).
3. J.Eickenmeier, R.Huhne, A.Guth et al., *Supercond. Sci. L.*, **23**, 085012 (2010).
4. H.L.Suo, Y.Zhao, M.Liu et al., *Supercond. Sci. Technol.*, **21**, 025005 (2008).
5. D.P.Rodionov, I.V.Gervasyeva, Ju.V.Khlebnikov et al., *Techn. Phys. Lett.*, **36**, 1 (2010).

6. N.Eliaz, T.M.Sridhar, E.Gileadi, *Electrochem. Acta*, **50**, 2893 (2005).
7. A.O.Ijodola, J.R.Thomson, A.Goyal et al., *Physica C*, **403**, 163 (2004).
8. Y.A.Ganenko, H.Rauh, P.Kruger, *Appl. Phys. Lett.*, **98**, 152303 (2011).
9. M.-W.Kim, B.-H.Jun, B.Ki Ji et al., *J. Korean Powder Met. Inst.*, **14**, 13 (2007).
10. P.P.Bhattacharjee, R.K.Ray, A.Upadhyaya, *Mater. Sci. Eng. A*, **488**, 84 (2008).
11. M.M.Gao, H.L.Suo, P.K.Gao et al., *J. Phys.: Conf. Series*, **234**, 022010 (2010).
12. H.Sakamoto, Y.Nagasu, Y.Ohashi et al., *Physica C*, **463–465**, 600 (2007).
13. C.C.Clickner, J.W.Ekin, N.Cheggour et al., *Cryogenics*, **46**, 432 (2006).
14. C.Cantoni, A.Goyal. X.Li et al., *IEEE Trans. Appl. Supercond.*, **15**, 2981 (2005).
15. J.Xiong, V.Matias, H.Wang et al., *J. Appl. Phys.*, **108**, 083903 (2010).
16. F.P.Larkins, P.J.Fensham, *Nature*, **215**, 1268 (1967).
17. V.A.Finkel, L.P.Degtyarenko, V.V.Derevyanko et al., *Problems Atom Sci. & Techn. Series of Rad. Effects & Rad. Metal Sci.*, No.4, 169 (2006).
18. F.H.Elinger, W.P.Sykes, *Trans. Am. Soc. Met.*, **28**, 613 (1940).
19. A.M.Bovda, V.A.Bovda, V.V.Derevyanko et al., *J. Iron & Steel Inst.*, **19**, 92 (2006).
20. V.M.Azhazha, G.P.Brekharya, A.M.Bovda et al., *Problems Atom. Sci. & Techn. Series Vacuum, Pure Mater., Supercond.*, No.4, 154 (2007).
21. P.P.Bhattacharjee, R.K.Ray, N.Tsuji, *Metallurgy & Mater. Trans. A*, **41**, 285 (2010).
22. Y.X.Zhou, R.Naguih, H.Fang, K.Salama, *Supercond. Sci. Technol.*, **17**, 947 (2004).
23. R.E.Bolmaro, A.Roatia, A.L.Fourty et al., in: Proc. ICOTOM XII, August 9–13, Montreal, Canada (1999), p.316.
24. F.A.Mohamed, T.G.Longdon, *Metallurgical Trans. A*, **6**, 927 (1975).
25. I.I.Axenov, V.G.Padalka, A.N.Belokhvostikov et al., *Plasma Phys. and Control. Fusion*, **28**, 761 (1986).
26. I.I.Axenov, A.A.Andreev, A.A.Romanov et al., *Ukr. Phys. J.*, **24**, 515 (1979).
27. I.I.Axenov, V.M.Khoroshikh, *IEEE Trans. Plasma Sci.*, **27**, 1026 (1999).
28. V.M.Khoroshikh, S.A.Leonov, V.A.Belous, *Problems Atom. Sci. & Techn. Series Vacuum, Pure Mater., Supercond.*, No.1, 72 (2008).

Дослідження та розробки з отримання підкладок на основі сплавів Ni–W для ВТНП-провідників другого покоління

В.О.Фінкель, О.М.Бовда, В.В.Дерев'янко, С.О.Леонов, М.С.Сунгуров, Т.В.Сухарева, В.М.Хороших, Ю.М.Шахов

Вивчено можливості отримання високоякісних підкладок для ВТНП-провідників другого покоління на основі сплавів Ni–W у діапазоні концентрації вольфраму 0–9.5 at. %. Дослідження і розробки проводилися в наступних основних напрямах: а) синтез сплавів Ni–W, б) отримання стрічки із сплавів Ni–W шляхом плющення і подальшої термообробки, в) нанесення буферного шару TiN на поверхню стрічки. Вперше встановлено можливість отримання кубічної текстури {001} <100>, що сприяє подальшому епітаксійному зростанню шарів надпровідника $YBa_2Cu_3O_{7-\delta}$ на поверхні стрічки з парамагнітних сплавів Ni–W з високим вмістом вольфраму шляхом зміни режимів нанесення покриттів на основі TiN.